EUROFUSION WPJET1-PR(15) 14445

H Urano et al.

Origin of Edge Transport Barrier Expansion with Edge Poloidal Beta at Large Shafranov Shift in ELMy H-mode Plasmas

Preprint of Paper to be submitted for publication in Physical Review Letters

This work has been carried out within the framework of the EUROfusion Consortium and has received funding from the Euratom research and training programme 2014-2018 under grant agreement No 633053. The views and opinions expressed herein do not necessarily reflect those of the European Commission.

This document is intended for publication in the open literature. It is made available on the clear understanding that it may not be further circulated and extracts or references may not be published prior to publication of the original when applicable, or without the consent of the Publications Officer, EUROfusion Programme Management Unit, Culham Science Centre, Abingdon, Oxon, OX14 3DB, UK or e-mail Publications.Officer@euro-fusion.org

Enquiries about Copyright and reproduction should be addressed to the Publications Officer, EUROfusion Programme Management Unit, Culham Science Centre, Abingdon, Oxon, OX14 3DB, UK or e-mail Publications.Officer@euro-fusion.org

The contents of this preprint and all other EUROfusion Preprints, Reports and Conference Papers are available to view online free at http://www.euro-fusionscipub.org. This site has full search facilities and e-mail alert options. In the JET specific papers the diagrams contained within the PDFs on this site are hyperlinked

Origin of Edge Transport Barrier Expansion with Edge Poloidal Beta at Large Shafranov Shift in ELMy H-mode Plasmas

H. Urano[1], S. Saarelma[2], L. Frassinetti[3], C.F. Maggi[2], I. Lupelli[2], M. Leyland[4], M. Beurskens[5], I.T. Chapman[2], C. Challis[2], C. Perez von Thun[6], C. Giroud[2], S. Pamela[2] and JET Contributors[†]
EUROfusion Consortium, JET, Culham Science Centre, Abingdon, OX14 3DB, UK
[1]*Japan Atomic Energy Agency, Naka Fusion Institute, Naka, Ibaraki 311-0193 Japan*
[2]*Culham Centre for Fusion Energy, Culham Science Centre, Abingdon OX14 3DB, UK*
[3]*Division of Fusion Plasma Physics, KTH Royal Institute of Technology, Stockholm, Sweden*
[4]*York Plasma Institute, University of York, Heslington, York, YO10 5DD, UK*
[5]*Max-Planck-Institut für Plasmaphysik, Wendelsteinstr. 1, D-17491, Greifswald, Germany*
[6]*Forschungszentrum Jülich, Institut für Energie- und Klimaforschung 4, D-52425, Jülich, Germany*
[†]*See the Appendix of F. Romanelli et al., Proc. 25th IAEA FEC 2014, St Perersburg, Russia*
(Dated: October 8, 2015)

The origin of edge transport barrier (ETB) expansion with edge poloidal beta was examined involving the edge and core interplay in ELMy H modes. The ETB expansion with edge poloidal beta is accompanied by increased edge pressure gradient. This MHD stability improvement of edge pressure gradient is attributed to the increase of the Shafranov shift, which gives approximately the proportionality between ETB width and the square root of edge poloidal beta. An experimentally observed dependence of ETB width on edge poloidal beta originates from the displacement of the edge MHD stability boundary due to the stabilization effect induced by the Shafranov shift.

PACS numbers: 28.52.-s, 52.25.-b, 52.55.-s, 52.55.Fa, 52.55.Tn

The formation of an edge transport barrier (ETB) in H modes [1] reduces significantly heat and particle transport in the barrier region. This stair-step like profiles in density and temperature at the plasma edge lead to an overall confinement enhancement of fusion devices in contrast to a normal regime (L mode). The H mode is generally accompanied by the appearance of pulsating plasma heat and particle losses called edge localized modes (ELMs) [2]. ELM bursts generally originate from ideal magnetohydrodynamic (MHD) instability against a coupled peeling-ballooning mode (PBM) driven by an edge pressure gradient and a bootstrap current [3, 4]

The projected fusion performance is correlated with the pressure at the ETB top [5]. This is because core plasma temperature depends strongly on the temperature at the ETB top through the profile resilience [6]. Moreover, the increase in global poloidal beta β_p or Shafranov shift improves the edge PBM stability limit and enables the edge pressure gradient to grow further [7–9]. Thus, the proportionality between global and edge poloidal beta values holds at a given magnetic geometry. In the present understanding, the edge and core interplay of this virtuous cycle determines the overall confinement in ELMy H mode plasmas [10].

For the interest of predicting the fusion gain in a future reactor, the experimental characterization of the ETB structure has been addressed intensively. It has been widely recognized that the ETB width Δ_ped at the pre-ELM state expands with the edge poloidal beta value as [11–15]:

$$\Delta_\mathrm{ped} \propto {\beta_\mathrm{p,ped}}^{\xi} \quad (\xi \simeq 0.5) \tag{1}$$

where the exponent ξ is generally close to 0.5. However, little is known about the origin of the physics responsible for this relationship between Δ_ped and $\beta_\mathrm{p,ped}$ obtained in ELMy H modes. An understanding of the physics process characterizing the ETB width is of the utmost importance to clarify a completed system of the ETB structure. The modelling of the ETB spatial structure requires the experimental evidence and a reliable theoretical physics picture for an accurate prediction towards ITER.

This Letter presents the origin of ETB expansion with $\beta_\mathrm{p,ped}$ as a part of the self-consistent physics picture of the edge and core interplay in ELMy H modes. To accomplish this study, a data set of ELMy H mode plasmas with varying the neutral beam (NB) heating power in the JET tokamak has been analyzed. The ETB profile can simply be characterised geometrically by three components of width, gradient and height. Hereafter, Δ_ped represents the ETB width in the normalized poloidal flux space. If the ETB width is expressed by $\Delta_\mathrm{ped} \propto {\beta_\mathrm{p,ped}}^{\xi}$ with varying the heating power while the other experimental conditions are fixed, then the edge pressure gradient is given by:

$$\left(\frac{\mathrm{d}p}{\mathrm{d}\psi}\right)_\mathrm{ped} \simeq \frac{\beta_\mathrm{p,ped}}{\Delta_\mathrm{ped}} \cdot \frac{B_\mathrm{p}^2}{2\mu_0} \propto \frac{\beta_\mathrm{p,ped}}{{\beta_\mathrm{p,ped}}^{\xi}} = {\beta_\mathrm{p,ped}}^{1-\xi} \tag{2}$$

where B_p and μ_0 denote the edge poloidal magnetic field strength and the permeability in vacuum, respectively. Thus, the origin of the relationship between Δ_ped and $\beta_\mathrm{p,ped}$ is essentially synonymous with the origin of the relationship between $(\mathrm{d}p/\mathrm{d}\psi)_\mathrm{ped}$ and $\beta_\mathrm{p,ped}$ through the exponent ξ.

The experiments were conducted at a plasma current $I_\mathrm{p} = 1.4$ MA and a toroidal magnetic field $B_\mathrm{t} = 1.7$ T at a

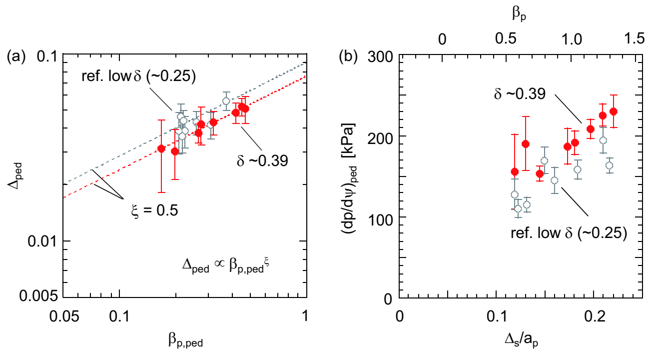

FIG. 1. (a) The ETB width $\Delta_{\rm ped}$ as a function of $\beta_{\rm p,ped}$ at 1.4MA/1.7T. (b) Dependence of the ETB pressure gradient $({\rm d}p/{\rm d}\psi)_{\rm ped}$ on the Shafranov shift $\Delta_{\rm s}/a_{\rm p}$ (or $\beta_{\rm p}$).

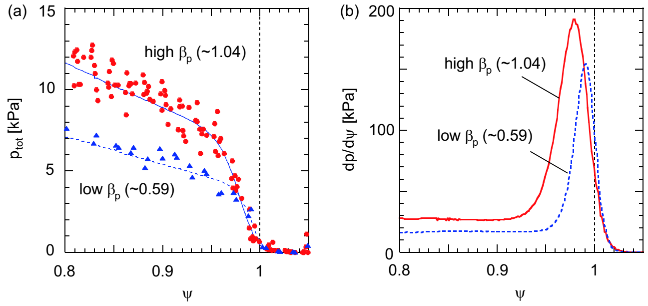

FIG. 2. Edge profiles of (a) the total pressure $p_{\rm tot}$ and (b) the pressure gradient ${\rm d}p/{\rm d}\psi$ for low and high $\beta_{\rm p}$ cases at $\delta = 0.39$.

given magnetic geometry with an ellipticity $\kappa = 1.6-1.7$, a triangularity $\delta = 0.39$ and a safety factor at 95% flux surface $q_{95} \simeq 3.9$ [16, 17]. The NB heating power applied in the range of $5-16$MW was sufficient to change $\beta_{\rm p,ped}$ from 0.17 to 0.45.

Fig. 1(a) shows the dependence of $\Delta_{\rm ped}$ on $\beta_{\rm p,ped}$ in this series of experiments. The data in low $\delta(= 0.25)$ case is also plotted as a reference. The ETB width scales approximately as ${\beta_{\rm p,ped}}^{1/2}$. Fig. 1(b) shows the ETB pressure gradient at the maximum $({\rm d}p/{\rm d}\psi)_{\rm ped}$ as a function of the Shafranov shift normalized to the minor radius $\Delta_{\rm s}/a_{\rm p}$. The $({\rm d}p/{\rm d}\psi)_{\rm ped}$ increases continuously with the Shafranov shift. Fig. 2 shows the edge profiles of the total pressure and the pressure gradient at the pre-ELM state for two cases of $\beta_{\rm p}$ of 0.59 ($\Delta_{\rm s}/a_{\rm p} = 11.9\%$) and 1.04 ($\Delta_{\rm s}/a_{\rm p} = 18.0\%$) at $\delta = 0.39$. When the Shafranov shift is increased, the ETB expands radially more inward from 0.031 to 0.043 together with the increase of $\beta_{\rm p,ped}$ from 0.17 to 0.32. Moreover, it is noted that the peak pressure gradient in the ETB region becomes larger from 160kPa to 190kPa at the same time.

Figs. 3(a) and (b) show the distribution of the local magnetic shear $S_{\rm l}$ [18] on a poloidal cross section evaluated by EFIT++ [19] for the pair of plasmas in Fig. 2. When the Shafranov shift is increased, the edge $S_{\rm l}$ becomes stronger only at the low field side (LFS). Fig. 3(c) shows the edge profiles of $S_{\rm l}$ at the LFS at $Z = Z_{\rm axis}$. The peak $S_{\rm l}$ is raised from -0.24 m^{-1} to -0.53 m^{-1} with increased $\Delta_{\rm s}/a_{\rm p}$ as a consequence of the self-consistent edge and core interplay. Since the toroidal magnetic effect plays a key role in the ballooning mode, this mode is stabilized by the increased $S_{\rm l}$ in the bad curvature region together with the magnetic well effect due to a shortened connection length in this region [20, 21].

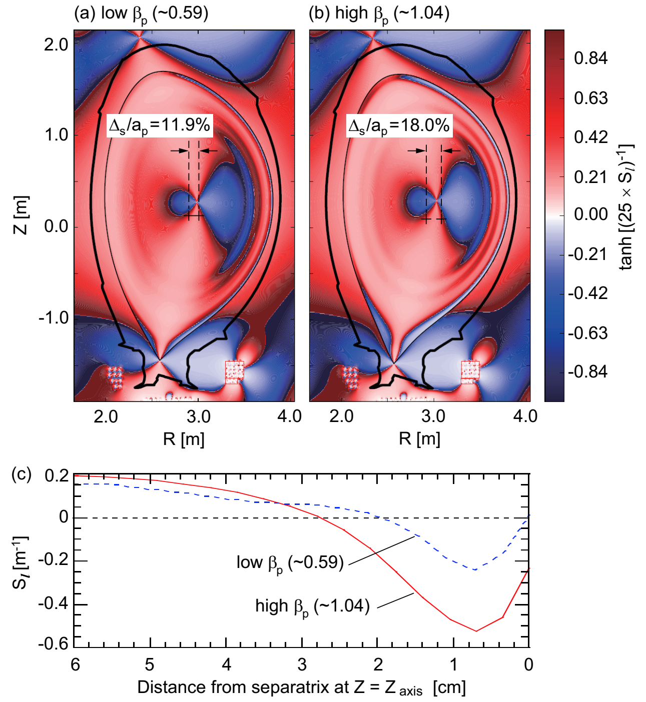

FIG. 3. Contours of local magnetic shear $S_{\rm l}$ for (a) low and (b) high $\beta_{\rm p}$. (c) Edge $S_{\rm l}$ profiles at the low field side at $Z = Z_{\rm axis}$.

Fig. 4 shows the edge PBM stability boundary calculated by ELITE [22] for the pair of plasmas in Fig. 2. The normalized pressure gradient is defined as $\alpha = -(\mu_0/2\pi^2)({\rm d}p/{\rm d}\psi)({\rm d}V/{\rm d}\psi)(V/2\pi^2 R)^{1/2}$, where V and R denote the plasma volume in each flux surface and the major radius, respectively. The stability limit of the edge pressure gradient is raised by the stabilization effect of the Shafranov shift consistently with the experiment. The values of $({\rm d}p/{\rm d}\psi)_{\rm ped}$ and $\beta_{\rm p,ped}$ self-consistently marginal against the PBM are 130 kPa and 0.15 at low $\beta_{\rm p}$ and 180 kPa and 0.29 at high $\beta_{\rm p}$, respectively. Assuming $({\rm d}p/{\rm d}\psi)_{\rm ped} \propto {\beta_{\rm p,ped}}^{\eta}$, the exponent $\eta_{\rm PBM}$ obtained at the PBM stability boundary is given as:

$$\eta_{\rm PBM} = \frac{\ln\left({({\rm d}p/{\rm d}\psi)_{\rm ped}}^{\rm h}/{({\rm d}p/{\rm d}\psi)_{\rm ped}}^{\rm l}\right)}{\ln\left({\beta_{\rm p,ped}}^{\rm h}/{\beta_{\rm p,ped}}^{\rm l}\right)} \qquad (3)$$

where the superscripts l and h indicate the low and high $\beta_{\rm p}$ cases, respectively. Substituting $({\rm d}p/{\rm d}\psi)_{\rm ped}$ and $\beta_{\rm p,ped}$ marginal to the PBM into Eq. (3), one obtains $\eta_{\rm PBM} \simeq 0.5$. From the geometric property shown in

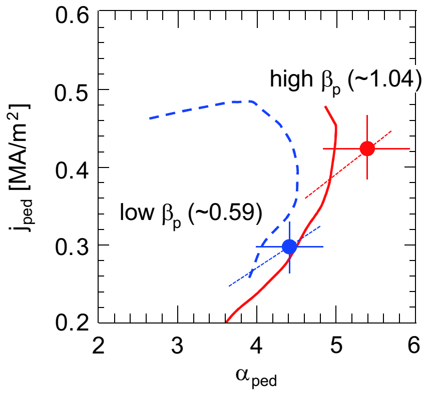

FIG. 4. Edge PBM stability boundary in a $(j_{\rm ped}, \alpha_{\rm ped})$ space for low and high global $\beta_{\rm p}$ cases at $\delta = 0.39$.

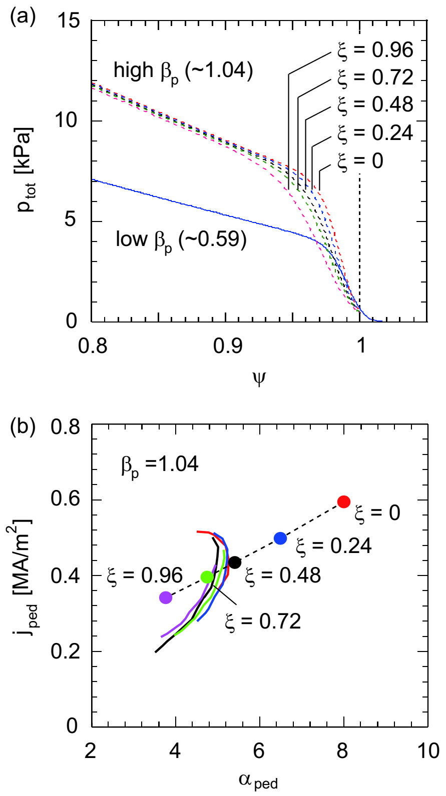

FIG. 5. (a) Edge profiles of the total pressure $p_{\rm tot}$ for the variation of the ETB width. (b) Edge PBM stability diagram for the variation of the ETB width.

Eq. (2), the displacement of the stability limit due to the Shafranov shift is expressed as $\Delta_{\rm ped} \propto \beta_{\rm p,ped}{}^{1-\eta} \simeq \beta_{\rm p,ped}{}^{0.5}$. This is similar to the one obtained experimentally.

Further detailed analysis is shown in Fig. 5. The ETB width is artificially varied for the high $\beta_{\rm p}$ case by changing the exponent ξ in the function form of $\Delta_{\rm ped} \propto \beta_{\rm p,ped}{}^{\xi}$ against low $\beta_{\rm p}$ case with the self-consistent marginally stable pressure profile (see Fig. 5(a)). It is noted that

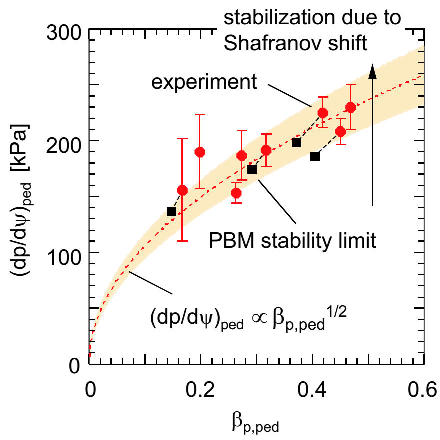

FIG. 6. The pressure gradient in the ETB region $({\rm d}p/{\rm d}\psi)_{\rm ped}$ as a function of $\beta_{\rm p,ped}$. Shaded area indicates $({\rm d}p/{\rm d}\psi)_{\rm ped} \propto \beta_{\rm p,ped}{}^{1/2}$ within the error of $\pm 10\%$.

in the variation of ξ from 0 to 0.96 the PBM stability boundaries are approximately the same for all the cases because the stabilization effect of the Shafranov shift is the same due to a fixed global $\beta_{\rm p}$ (see Fig. 5(b)). At $\xi = 0$ where the ETB width is independent of $\beta_{\rm p,ped}$, the ETB is very unstable because of its too steep peak pressure gradient. With increased ξ, the operational point at the steepest pressure gradient strides over the stability boundary due to the reduction in the pressure gradient. The consistency to the PBM stability boundary holds at the exponent ξ of $0.5 - 0.7$ in $\Delta_{\rm ped} \propto \beta_{\rm p,ped}{}^{\xi}$.

Fig. 6 shows $({\rm d}p/{\rm d}\psi)_{\rm ped}$ as a function of $\beta_{\rm p,ped}$ for the values measured and for the values evaluated at the MHD stability limit. The experimental data show the relationship of $({\rm d}p/{\rm d}\psi)_{\rm ped} \propto \beta_{\rm p,ped}{}^{1/2}$. The values of $({\rm d}p/{\rm d}\psi)_{\rm ped}$ and $\beta_{\rm p,ped}$ marginal to the stability limit approximately follows the experimental values. Since $\Delta_{\rm ped} \propto \beta_{\rm p,ped}{}^{\xi}$ is equivalent to $({\rm d}p/{\rm d}\psi)_{\rm ped} \propto \beta_{\rm p,ped}{}^{1-\xi}$ as described earlier, this result is indicative that the proportionality between the ETB width $\Delta_{\rm ped}$ and $\beta_{\rm p,ped}{}^{1/2}$ originates from the stabilization effect due to the Shafranov shift, which increases the edge pressure gradient as shown in Fig. 1(b).

In discussion, two lines of supportive evidence are provided for cases where $\Delta_{\rm ped} \propto \beta_{\rm p,ped}{}^{1/2}$ is not satisfied. First, in contrast to many other tokamaks, the ETB width does not scale as $\beta_{\rm p,ped}{}^{1/2}$ but as $\beta_{\rm p,ped}{}^{1}$ in NSTX [23]. The stabilization due to the Shafranov shift extends the edge MHD stability boundary only at the ballooning component of the PBM [7–9, 20, 21]. Differently from other tokamaks, the ETB in NSTX generally reaches a low n kink/peeling mode boundary far away from the coupled region of the PBM boundary [24] where the stabilization due to the Shafranov shift is not effective. If there is no stabilization effect on $({\rm d}p/{\rm d}\psi)_{\rm ped}$, then one can obtain $\Delta_{\rm ped} \propto \beta_{\rm p,ped}/({\rm d}p/{\rm d}\psi)_{\rm ped} \sim \beta_{\rm p,ped}$. Therefore, it follows that the ETB width expands linearly with

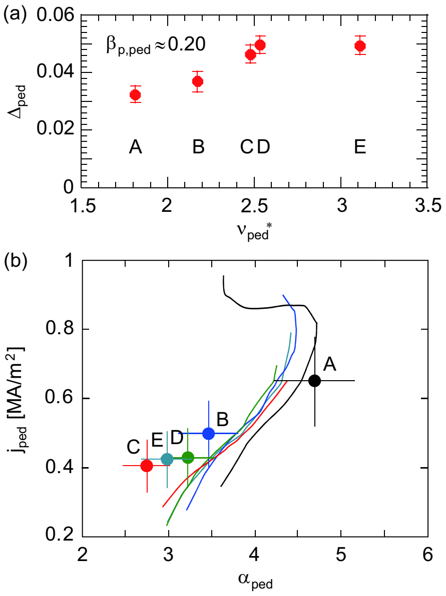

FIG. 7. (a) Dependence of $\Delta_{\rm ped}$ on the collisionality at the steepest pressure gradient $\nu^*_{\rm ped}$ at 2.5MA/2.6T. (b) Edge PBM stability diagram in this series of experiments.

$\beta_{\rm p,ped}$ in a situation where the ETB is destabilized by a purely low n kink/peeling mode.

Second, one can also expand this physics picture to the case at fixed pressure at the ETB top or $\beta_{\rm p,ped}$. In this case, one obtains $\Delta_{\rm ped} \propto ({\rm d}p/{\rm d}\psi)_{\rm ped}{}^{-1}$, indicating that $\Delta_{\rm ped}$ is inversely proportional to the pressure gradient achievable against the edge MHD stability. The edge pressure gradient is raised at high δ by the improvement of the PBM stability (see Fig. 1(b)). Then, relatively a narrower ETB width at high δ is expected in comparison with low δ at a given $\beta_{\rm p,ped}$. This is proven to be consistent with the experiments as shown in Fig. 1(a). Besides, the ETB broadening at fixed $\beta_{\rm p,ped}$ has been observed at high collisionality with increased gas fuelling rate in JET [25–28] and JT-60U [29]. Fig. 7(a) shows the expansion of $\Delta_{\rm ped}$ with the collisionality at the steepest pressure gradient $\nu^*_{\rm ped}$ in the JET experiments at 2.5MA/2.6T with a deuterium gas rate scan while $\beta_{\rm p,ped}$ is kept at ~ 0.20 [26]. Fig. 7(b) shows the edge PBM stability diagram at the toroidal mode number $n \leq 70$ in this series of experiments. In the variation of $\nu^*_{\rm ped}$ the PBM stability boundaries are nearly the same for all the cases at a constant global $\beta_{\rm p}$ of ~ 0.5, so that the stabilization effect of the Shafranov shift is the same. The experimental edge pressure gradient decreases approximately along the stability boundary with the reduction in $j_{\rm ped}$, which destabilizes a shorter wavelength ballooning mode roughly with the increase of $\nu^*_{\rm ped}$. Hence, this reduction of the edge pressure gradient always accompanies the ETB broadening with increased $\nu^*_{\rm ped}$ at fixed $\beta_{\rm p,ped}$.

For the prediction of the ETB structure, the EPED model has recently been developed based on $\Delta_{\rm ped} \propto \beta_{\rm p,ped}{}^{1/2}$ [12, 30]. This model assumes that the relationship between $\Delta_{\rm ped}$ and $\beta_{\rm p,ped}$ originates from the kinetic ballooning mode during the inter-ELM phase. On the other hand, this is an empirical scaling law constructed only from the pre-ELM pressure profiles. Thus, there is an illogical leap in the explanation of the evolution of the ETB width during the inter-ELM phase based on this scaling law. In contrast, it is convincing that the ETB expansion with $\beta_{\rm p,ped}$ at the pre-ELM state marginal to the stability limit corresponds to the displacement of the edge MHD stability boundary and the trajectory along the stability boundary. The scaling law of $\Delta_{\rm ped} \propto \beta_{\rm p,ped}{}^{1/2}$ was obtained because the experiments were conducted for the variation of $\beta_{\rm p,ped}$ in which the stabilization effect of the Shafranov shift worked. That is why this scaling law is only applicable to cases in which the ETB is marginal to the intermediate n peeling-ballooning mode.

In summary, the origin of ETB expansion with $\beta_{\rm p,ped}$ was examined involving the self-consistent physics picture of the edge and core interplay in ELMy H modes. From the geometric property, the relationship of $\Delta_{\rm ped} \propto \beta_{\rm p,ped}{}^{\xi}$ is essentially equivalent to $({\rm d}p/{\rm d}\psi)_{\rm ped} \propto \beta_{\rm p,ped}{}^{1-\xi}$. The ETB expansion with $\beta_{\rm p,ped}$ is always accompanied by the increase of $({\rm d}p/{\rm d}\psi)_{\rm ped}$ expressed as $({\rm d}p/{\rm d}\psi)_{\rm ped} \propto \beta_{\rm p,ped}{}^{1/2}$. This PBM stability improvement of $({\rm d}p/{\rm d}\psi)_{\rm ped}$ is attributed to the increase of the Shafranov shift. The consistency to the MHD stability boundary holds at the exponent ξ of $0.5-0.7$ in $\Delta_{\rm ped} \propto \beta_{\rm p,ped}{}^{\xi}$. These results lead to the conclusion that the ETB expansion with $\beta_{\rm p,ped}$ arises from the stabilization effect of the Shafranov shift. This leaves the next question open to explore about how $\beta_{\rm p,ped}$ is determined at the pre-ELM state. In experiments, dependence of ETB width on $\beta_{\rm p,ped}$ has been examined by progressively controlling $\beta_{\rm p,ped}$. An investigation of a physics picture of the ETB structure in conjunction with the peak pressure gradient and the current density marginal to the edge MHD stability limit given by the magnetic geometry and the stabilization effect of the Shafranov shift will be the subject of a future study.

The authors are grateful to Drs. Y. Kamada, T. Donne, L.D. Horton and D. Borba for their encouragement. The first author (H. Urano) thanks Dr. N. Aiba for theoretical discussion on the edge MHD stability. This work has been carried out within the framework of the EUROfusion Consortium and has received funding from the Euratom research and training programme 2014-2018 under grant agreement No 633053. The views and opinions expressed herein do not necessarily reflect those of the European Commission.

[1] F. Wagner *et al*, Phys. Rev. Lett. **49**, 1408 (1982).

[2] H. Zohm, Plasma Phys. Control. Fusion **38**, 105 (1996).
[3] H.R. Wilson *et al*, Phys. Plasmas **6**, 1925 (1999).
[4] P.B. Snyder *et al*, Nucl. Fusion **44**, 320 (2004).
[5] J. Kinsey *et al*, Nucl. Fusion **51**, 083001 (2011).
[6] X. Garbet *et al*, Plasma Phys. Control. Fusion **46**, 1351 (2004).
[7] N. Aiba *et al*, Nucl. Fusion **54**, 114007 (2014).
[8] I.T. Chapman *et al*, Nucl. Fusion **55**, 013004 (2015).
[9] J. Simpson *et al*, submitted to Plasma Phys. Control. Fusion.
[10] H. Urano *et al*, Nucl. Fusion **54**, 116001 (2014).
[11] H. Urano *et al*, Nucl. Fusion **48**, 045008 (2008).
[12] P.B. Snyder *et al*, Phys. Plasmas **16**, 056118 (2009).
[13] M. Beurskens *et al*, Phys. Plasmas **18**, 056120 (2011).
[14] A. Kirk *et al*, Plasm Phys. Control. Fusion **51**, 065016 (2009).
[15] J.R. Walk *et al*, Nucl. Fusion **52**, 063011 (2012).
[16] C. Challis *et al*, Nucl. Fusion **55**, 053031 (2015).
[17] C.F. Maggi *et al*, Nucl. Fusion (in press).
[18] P.J. Mc Carthy *et al*, Plasm Phys. Control. Fusion **55**, 085011 (2013).
[19] M. Fitzgerald *et al*, Nucl. Fusion **53**, 113040 (2013).
[20] M.S. Chance, S.C. Jardin, and T.H. Stix, Phys. Rev. Lett. **51**, 1963 (1983).
[21] H.R. Wilson *et al*, Phys. Plasmas **6**, 873 (1999).
[22] H.R. Wilson *et al*, Phys. Plasmas **9**, 1277 (2002).
[23] A. Diallo *et al*, Nucl. Fusion **53**, 093026 (2013).
[24] R. Groebner *et al*, Nucl. Fusion **53**, 093024 (2013).
[25] M. Beurskens *et al*, Plasm Phys. Control. Fusion **55**, 124043 (2013).
[26] M. Leyland *et al*, Nucl. Fusion **55**, 013019 (2015).
[27] C. Giroud *et al*, Plasm Phys. Control. Fusion **57**, 035004 (2015).
[28] L. Frassinetti *et al*, Proc. 42nd Eur. Conf. Plasma Phys. (Lisbon, Portugal) EPS, Geneva P2.130 (2015).
[29] H. Urano *et al*, Proc. 42nd Eur. Conf. Plasma Phys. (Lisbon, Portugal) EPS, Geneva P5.146 (2015).
[30] P.B. Snyder *et al*, Nucl. Fusion **51**, 103016 (2011).